value of the parameter ξ (*i.e.* the ratio of the sample-to-detector flight path and the total flight path), the differential cross section measured in TOF neutron diffractometry. (*b*) For coherent inelastic scattering, this cross section is fully described by the scattering surface in the four-dimensional space ($\mathbf{Q}_e$, ω). (*c*) For scattering by low-frequency acoustic phonons, this surface is defined at every point of the space $\mathbf{Q}_e$ if $\beta < \beta_\nu$ but it is not defined in some regions of this space if $\beta > \beta_\nu$. (*d*) Forbidden ranges exist in both incident wavelengths and scattering angles if $\beta_\nu < \beta < \beta_\mu$; in these ranges, the scattering is allowed if $\beta > \beta_\mu$. (*e*) The value of β_μ depends on the orientation of the scanning plane in the space $\mathbf{Q}_e$. For the particular case of scanning at constant offset from the Bragg scattering angle, β_μ becomes $1/\cos\theta_B$, as reported by Willis (1986). (*f*) Finally, we have found an analytical expression for the differential cross section of scattering by low-energy acoustic phonons. This will be used in a further paper to calculate the TDS correction of the Bragg peaks measured by the TOF diffractometer.

The authors are deeply indebted to Dr C. J. Carlile of the Rutherford Appleton Laboratory, England, for discussions on the contents of this paper.

References

CARLILE, C. J., KEEN, D. A., WILSON, C. C. & WILLIS, B. T. M. (1992). *Acta Cryst.* A**48**, 826–829.
COOPER, M. J. (1971). *Acta Cryst.* A**27**, 148–157.
COOPER, M. J. & ROUSE, K. D. (1968). *Acta Cryst.* A**24**, 405–410.
MARSHALL, W. & LOVESEY, S. W. (1971). *Theory of Thermal Neutron Scattering*. Oxford: Clarendon Press.
POPA, N. C. (1987). Preprint JINR, No. E14-87-180. Joint Institute for Nuclear Research, Dubna, Russia.
WILLIS, B. T. M. (1969). *Acta Cryst.* A**25**, 277–300.
WILLIS, B. T. M. (1970). *Acta Cryst.* A**26**, 396–401.
WILLIS, B. T. M. (1986). *Acta Cryst.* A**42**, 514–525.

Acta Cryst. (1994). A**50**, 63–68

The Half-Widths of Powder Bragg Intensity Profiles Deduced in Reciprocal Space. I. Ideal Powders

BY ELISABETH ROSSMANITH

Mineralogisch-Petrographisches Institut der Universität Hamburg, D-2000 Hamburg 13, *Grindelallee* 48, *Germany*

(*Received* 30 *March* 1993; *accepted* 29 *June* 1993)

Abstract

New formulas for the full widths at half-maxima (FWHMs) of powder Bragg intensity profiles are deduced in reciprocal space, using the concept for the calculation of the peak width introduced for single-crystal diffractometry by Rossmanith [*Acta Cryst.* (1992), A**48**, 596–610]. In paper I, a basic formula for strain-free and preferred-orientation-free powders is deduced. Furthermore, it is shown that comparison of experimental widths with theoretical FWHMs calculated with the new expression results in physically significant values for the particle size in the powder. In a forthcoming paper II, the effect of strain on the FWHM will be analysed.

Introduction

Profile analysis of powder diffraction diagrams requires knowledge of the height, width and distribution function (*i.e.* Gauss, Lorentz, pseudo-Voigt *etc.*) of the intensity profile.

Expressions for the calculation of the resolution functions of *N*-crystal powder spectrometers are given by, for example, Sabine (1987) and Wroblewski (1991). The formulas given by these authors are difficult to handle for two reasons. First, most of the transmission and reflection probability distributions involved in the expressions are not known exactly in routine powder diffraction experiments. Second, evaluation of these expressions requires time-consuming computations of integrals, even if approximations (for example pseudo-Voigt) for the distribution functions are used.

The widths of the Bragg intensity profiles are, therefore, usually calculated using the simplified version of the formula given by Caglioti, Paoletti & Ricci (1958):

$$\Delta 2\theta^2 = U\tan^2\theta + V\tan\theta + W. \qquad (1a)$$

In Rietveld analysis (Rietveld, 1969), the physically meaningless half-width parameters U, V and W are determined by least-squares fitting of calculated to measured FWHMs.

Rossmanith (1992) introduced a new concept for the calculation of the widths of Bragg intensity profiles for single and multiple diffraction in single-crystal diffractometry. In this paper and in Rossmanith (1993*a*), it is shown that, with representation of the half-width parameters $\Delta\lambda/\lambda$ (wavelength spread), δ (divergence), r (mosaic-block radius) and η (mosaic spread) as well as the experimental conditions of the diffraction in reciprocal space, the widths of the profiles for single and multiple diffraction can be obtained from purely geometrical considerations. In Rossmanith (1993*b*), the simple but very effective approximation

$$\Delta\theta_{\mathbf{h}} \simeq \pm\delta + (\Delta\lambda/\lambda)\tan\theta_{\mathbf{h}} + 2\lambda/(r\sin 2\theta_{\mathbf{h}}) + \eta$$
$$\simeq \delta[\pm 1 + (\tan\theta_{\mathbf{h}}/\tan\theta_M)] + 2\lambda/(r\sin 2\theta_{\mathbf{h}}) + \eta \quad (1b)$$

was derived for the width $\Delta\theta_{\mathbf{h}}$ of the Bragg intensity profile measured with a triple-crystal diffractometer at a synchrotron-radiation source in parallel (−) and antiparallel (+) arrangements of the crystal with respect to the monochromator. $\theta_{\mathbf{h}}$ and θ_M are the kinematical Bragg angles of the sample and monochromator, respectively, and λ is the wavelength. It was shown in Rossmanith, Werner, Kumpat, Ulrich & Eichhorn (1993) that, with this approximation, the fit of calculated to experimental widths results in physically significant and consistent half-width parameters. In Rossmanith, Adiwidjaja, Eck, Kumpat & Ulrich (1994), the successful application of the concept to multiple diffraction experiments is demonstrated.

It is shown below that the concept introduced successfully for single-crystal diffractometry can also be easily applied to powder diffractometry resulting in an expression similar, but not equivalent, to (1*b*).

The basic formula for the width of Bragg reflections deduced in reciprocal space

For ideal powders, *i.e.* for powders consisting of small ideally perfect strain-free and randomly oriented crystallites, the width of the Bragg intensity profile mainly depends on the wavelength spread $\Delta\lambda/\lambda$ and the divergence δ of the X-ray beam received by the counter and on the crystallite or coherent-domain size of the powder sample.

In Fig. 1, the geometry of powder diffraction in reciprocal space is shown. The representation of the characteristics of the X-ray beam is identical for single-crystal and powder diffraction. The wavelength range $\Delta\lambda = \lambda_1 - \lambda_2$ results in two limiting Ewald spheres with radii $r_1^* = 1/\lambda_1 = 1/(\lambda + \Delta\lambda/2)$ and $r_2^* = 1/\lambda_2 = 1/(\lambda - \Delta\lambda/2)$, both passing through the origin of reciprocal space. Owing to the divergence δ, two such limiting broadened Ewald spheres, inclined relative to each other by δ, have to be drawn.

For simplicity, it is assumed that the powder consists of ideally perfect spherical crystallites (coherent scattering domains), with a mean radius r that is small enough for absorption and extinction effects within the crystallites to be neglected.

For an arbitrary reflection **h**, the radius of the spherical particles can be expressed as $r = d_{\mathbf{h}}N_{\mathbf{h}}/2$, where $d_{\mathbf{h}}$ is the interplanar spacing of the reflecting planes and $N_{\mathbf{h}}$ is the number of planes in the sphere. In reciprocal space, $d_{\mathbf{h}}$ is represented by the vector **h** normal to the reflecting planes with length $d_{\mathbf{h}}^* = 1/d_{\mathbf{h}}$. Consequently, r is represented by a vector in the direction of **h** with length $\varepsilon = 2/(d_{\mathbf{h}}N_{\mathbf{h}}) = 1/r$. Because this is true for all directions **h** in direct space, the zero point of the reciprocal lattice is enlarged to a sphere with radius ε, being a mathematical point only in the case of $N_{\mathbf{h}} = \infty$. Because of the translational symmetry of the reciprocal lattice, the enlargement of the zero point results in an enlargement of all reciprocal points to 'lattice spheres' with a common radius ε (see also Rossmanith, 1992, § II.*A*.1.)

With a large number and completely random orientation of crystallites in the powder, the corresponding reciprocal-lattice spheres of the individual crystallites build up concentric spherical shells about the origin of the reciprocal lattice whose radii are the various possible reciprocal-lattice vectors $d_{\mathbf{h}}^*$. The

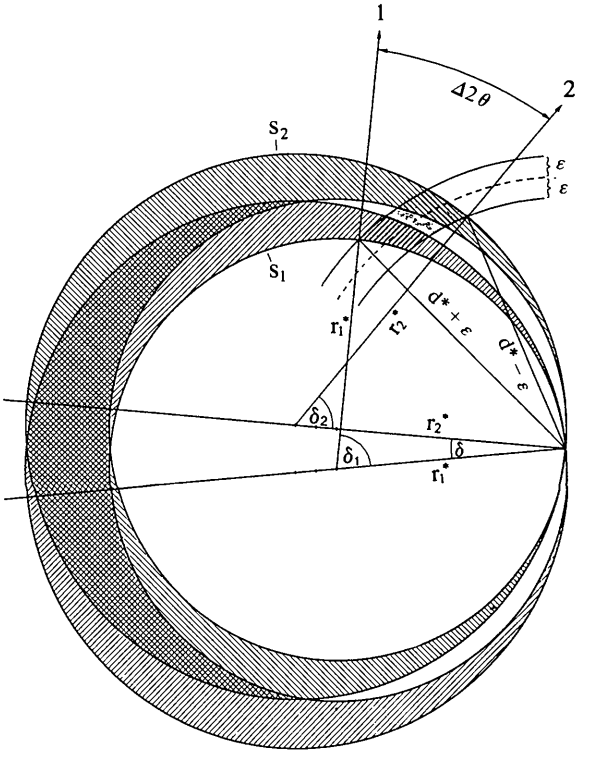

Fig. 1. The geometry of powder diffraction in reciprocal space.

thicknesses of the shells are consequently given by twice the radii ε of the individual 'lattice spheres' (Fig. 1).

The whole part of the shell, which lies between the two limiting spheres S_1 and S_2, is in a reflection position and contributes to the Bragg reflection. The corresponding intensity is reflected in all directions between the limiting rays 1 and 2 in Fig. 1. The maximum width of the Bragg intensity profile is therefore given by

$$\Delta 2\theta_{\mathbf{h}} = \delta_1 - \delta_2 + \delta, \tag{2a}$$

where

$$\delta_1 = 2 \arcsin [(d^*_{\mathbf{h}} + \varepsilon)/(2r^*_1)] \tag{2b}$$

$$\delta_2 = 2 \arcsin [(d^*_{\mathbf{h}} - \varepsilon)/(2r^*_2)] \tag{2c}$$

$$d^*_{\mathbf{h}} = 2 \sin \theta_{\mathbf{h}}/\lambda. \tag{2d}$$

$\theta_{\mathbf{h}}$ is the Bragg angle corresponding to the reflection $\mathbf{h}$, ε is a function of the crystallite radius r only and r^*_i depends solely on the wavelength and wavelength spread of the radiation used. For strain-free and preferred-orientation-free samples, (2), which is not at all difficult to calculate with the help of a computer, therefore represents the angular dependence of the width of the Bragg intensity profile as an explicit function of the wavelength and the width parameters $\Delta\lambda/\lambda$, δ and r.

The widths of the intensity profiles for special cases

(*a*) *Ideally monochromatic and parallel X-ray beam* ($\Delta\lambda/\lambda = \delta = 0$)

The angular dependence of the width on the crystallite size becomes apparent from Fig. 2. Because $\Delta\lambda = \delta = 0$, the X-ray beam is represented in reciprocal space by only one Ewald sphere. As in Fig. 1, the reciprocal 'lattice spheres' belonging to the individual randomly oriented crystallites of the powder coalesce into spherical shells, whose widths are determined by the crystallite size. With the assumption once more of spherical crystallites with radius r, the width of the shells is given by 2ε with $\varepsilon = 1/r = 2/(d_{\mathbf{h}}N_{\mathbf{h}}) = 2/(\mathbf{a}_i N_i)$, where the $\mathbf{a}_i$ are the lattice constants and the N_i are the numbers of unit cells in the crystal lying along the directions $\mathbf{a}_i$.

It is obvious from Fig. 2 that, for intermediate angles θ, the arc b given by

$$b = \Delta 2\theta_{\mathbf{h}}/(2\lambda) \tag{3a}$$

can be approximated by

$$b \simeq \varepsilon/\cos \theta_{\mathbf{h}}. \tag{3b}$$

From there, the approximation

$$\Delta 2\theta \simeq 2\varepsilon\lambda/\cos \theta_{\mathbf{h}} \tag{3c}$$

can be deduced for the width $\Delta 2\theta$, which can also be calculated from

$$\Delta 2\theta = \delta_1 - \delta_2 \tag{3d}$$

with

$$\delta_1 = 2 \arcsin [(d^*_{\mathbf{h}} + \varepsilon)\lambda/2]$$

$$\delta_2 = 2 \arcsin [(d^*_{\mathbf{h}} - \varepsilon)\lambda/2].$$

For comparison with an experiment, the relation between the width defined in (3*c*) and (3*d*) and the full width at half-maximum (FWHM) of an intensity profile has to be known.

If the kinematical approach, the intensity of coherent scattering of an ideally monochromatic and parallel incident beam from an ideally perfect small crystal is determined by

$$I^{\text{ideal}}_{\text{coh}} = I_e |F^2| G^2, \tag{3e}$$

where I_e is the intensity scattered by an electron and F is the structure factor. I_e and F are both slowly varying functions of θ. The intensity distribution function in (3*e*) is therefore determined by G^2, the exceedingly sharp interference function.

Deriving this function G^2, it is, for simplicity, convenient to consider the crystal as having the shape of a parallelepiped whose sides are parallel to the cell edges with the lengths $\mathbf{a}_i N_i$ (Azaroff, 1968,

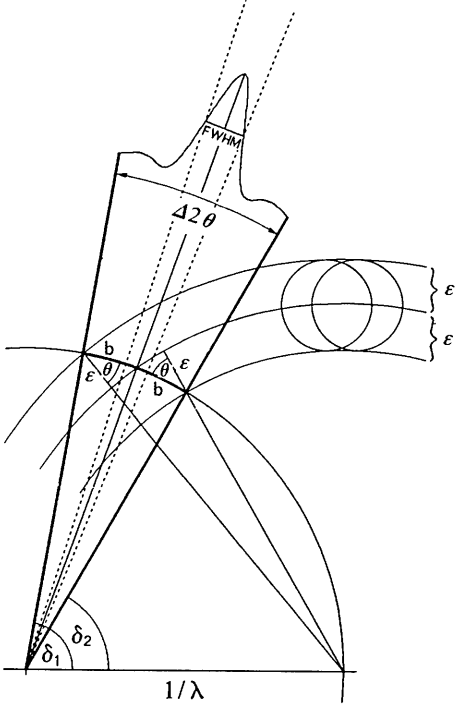

Fig. 2. The geometry of powder diffraction in reciprocal space: the special case $\Delta\lambda/\lambda = \delta = 0$.

formulas 9–24 and 9–25)

$$G^2 = \prod_i [\sin^2 N_i \mathbf{a}_i x\pi/(\sin^2 \mathbf{a}_i x\pi)]. \qquad (3f)$$

For such a crystal, $x = \varepsilon = 2/(\mathbf{a}_i N_i)$ corresponds to the second minimum of the oscillating function G^2 in the direction $\mathbf{a}_i$. The FWHM of the main maximum of G^2 is usually obtained by smoothing out the oscillating factors in $(3f)$ by exponential functions with the same maximum and area:

$$\sin^2 N_i \mathbf{a}_i x\pi/(\sin^2 \mathbf{a}_i x\pi) = N_i^2 \exp[-\pi(N_i \mathbf{a}_i x)^2]. \qquad (3g)$$

The corresponding half-width of the main maximum of G^2 in the direction $\mathbf{a}_i$ is therefore related to the width 2ε approximately by

$$2\varepsilon(\text{FWHM}) = [\ln 2/(4\pi)]^{1/2} 2\varepsilon. \qquad (3h)$$

It is usually assumed in standard textbooks that a very similar relation holds true for any direction and for crystals of any shape. Equation $(3h)$ is therefore inserted in $(3c)$, resulting in the Scherrer equation:

$$\Delta 2\theta(\text{FWHM}) = 0.94\lambda/(t_h \cos\theta_h), \qquad (3i)$$

where $t_h = 2r$ is the mean dimension of the crystallites normal to the reflecting plane.

In the second column of Table 1, the $\Delta 2\theta$(FWHM) calculated with $(3d)$ in connection with $(3h)$ for Cu $K\alpha_1$ radiation and $r = 300$ Å is given. It is easily shown that $(3i)$ yields identical results for all the Bragg angles considered in Table 1. Deviations between $(3i)$ and $(3d)$, $(3h)$ are observed only in the vicinity of $\theta_h = 90°$, *i.e.* at Bragg angles of no interest in powder diffractometry.

(b) Standard powder sample $(\varepsilon = 0)$ *and negligible divergence* $(\delta = 0)$

The geometrical conditions for this case are given in Fig. 3. The angles δ_1 and δ_2 agree with twice the Bragg angles of the two limiting wavelengths $\lambda \pm \Delta\lambda/2$. Using the FWHM of the wavelength spread for $\Delta\lambda$, the $\Delta 2\theta$(FWHM) results in

$$\Delta 2\theta(\text{FWHM}) = 2(\theta_1 - \theta_2), \qquad (4a)$$

with

$$\theta_1 = \arcsin[(\lambda + \Delta\lambda/2)/(2d_h)]$$

$$\theta_2 = \arcsin[(\lambda - \Delta\lambda/2)/(2d_h)]$$

$$d_h = \lambda/(2\sin\theta_h).$$

The width defined in $(4a)$ is given in the third column of Table 1. $\Delta\lambda/\lambda = 0.000306$, the value given by Ladell, Zagofsky & Pearlman (1975) for the FWHM of the characteristic Cu $K\alpha_1$ line, was used for calculation. Comparison of these widths with the values obtained with the expression

$$\Delta 2\theta(\text{FWHM}) = 2\Delta\lambda/\lambda \tan\theta_h \qquad (4b)$$

Table 1. *The peak width* $\Delta 2\theta$ *(FWHM)* (°) *calculated for* Cu $K\alpha_1$ *radiation*

$\Delta\lambda/\lambda = 0.000306$, $\delta = 0.05°$, $r = 300$ Å.

2θ	$\Delta 2\theta(r)$	$\Delta 2\theta(\Delta\lambda)$	$\Delta 2\theta(r, \Delta\lambda, \delta)$
20	0.140	0.006	0.197
40	0.147	0.013	0.210
60	0.160	0.020	0.230
80	0.180	0.029	0.260
100	0.215	0.042	0.307
120	0.276	0.061	0.387
140	0.404	0.096	0.550
160	0.796	0.199	1.045

indicates that, for the relevant Bragg-angle region, the two expressions yield identical results.

(c) Dependence on the divergence $(\varepsilon = \Delta\lambda/\lambda = 0)$

It is obvious from Fig. 1 that, for $\varepsilon = \Delta\lambda/\lambda = 0$, it follows that $\delta_1 = \delta_2$ and

$$\Delta 2\theta = \delta \qquad (5)$$

for all Bragg angles.

For diffractometers with a varying divergence for different Bragg angles, the constant δ in $(2a)$ and (5) must be replaced by the appropriate function $\delta = \delta(\theta)$.

(d) Derivation of an approximate expression for the FWHM

In the fourth column of Table 1, the full width at half-maximum calculated with (2) in connection with $(3h)$ for $\Delta\lambda/\lambda = 0.000306$, $\delta = 0.05°$ and $r = 300$ Å is given. It is easily proved that identical results can be obtained using the expression

$$\Delta 2\theta(\text{FWHM}) \simeq 2\Delta\lambda/\lambda \tan\theta_h + 0.94\lambda/(t_h \cos\theta_h) + \delta \qquad (6)$$

for all Bragg angles relevant in powder diffractometry.

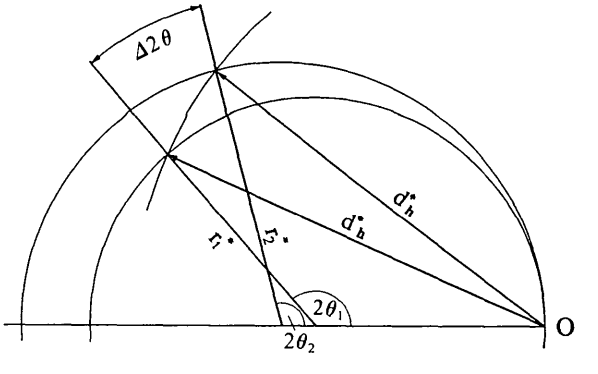

Fig. 3. The geometry of powder diffraction in reciprocal space: the special case $\varepsilon = \delta = 0$.

Application of the basic peak-width formula to an experiment

Experimental half-widths of ZnO and BaF_2 measured with Cu $K\alpha_1$ radiation are given in Fig. 3 and Table 1 of the paper of Langford, Boultif, Auffrédic & Louër (1993) and in Table 2 of the paper of Louër & Langford (1988), respectively. BaF_2 was used by these authors as standard powder for the determination of instrumental broadening. The particle size of the ZnO powder was obtained from transmission electron microscopy (TEM) by Bolis, Fubini, Giamello & Reller (1989), who state that the powder consists of 'agglomerates made up of crystallites ... in the range 300–600 Å and that the isolated crystallites of ZnO exhibit no well defined edges, but rather disc-like shapes'. It has been shown by Langford *et al.* (1993) that strain broadening is negligible for their BaF_2 and ZnO powder samples. The widths of ZnO as well as of BaF_2 are reproduced in Fig. 4 and in Tables 2 and 3 of this paper.

All three curves in Fig. 4 were calculated using the expressions (2) in connection with (3*h*) [expression (6) yields the same results], inserting for $\Delta\lambda/\lambda = 0.00306$ the FWHM of the characteristic Cu $K\alpha_1$ line and for $\delta = 0.05°$ the value given by Louër & Langford (1988) for the aperture of the receiving slit of the counter.

The best fit with the BaF_2 FWHM data (circles in Fig. 4) was obtained by inserting for the particle size (the coherent domain size) $t = 1$ μm, which is a typical value for a standard powder. The corresponding lowest curve in Fig. 4 matches the experimental widths very well. The small deviations between the experimental points and the curve, *i.e.* the shallow minimum of the measured width at $2\theta \sim 50°$ is probably because the divergence of the X-ray

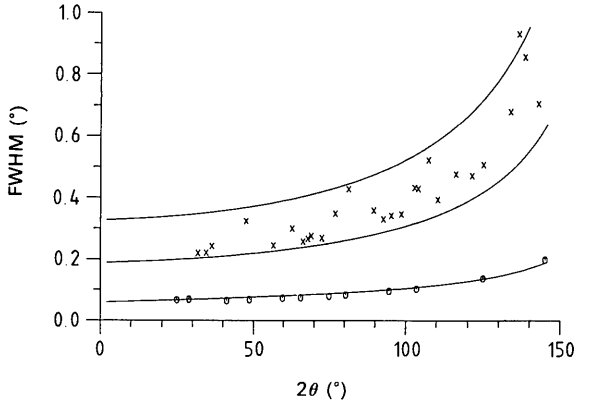

Fig. 4. Experimental and calculated FWHMs for Cu $K\alpha_1$ radiation. Curves calculated with $\Delta\lambda/\lambda = 0.000306$, $\delta = 0.05°$, $t = 1$ μm (lower curve), $t = 600$ Å (middle curve), $t = 300$ Å (upper curve). ○: experimental widths of BaF_2, X experimental widths of ZnO.

Table 2. *Experimental and calculated widths (FWHM) of* BaF_2 *(θ_h and widths in °)*

Cu $K\alpha_1$ radiation, $\Delta\lambda/\lambda = 0.000306$, $\delta = 0.05°$, $t = 1$ μm.

h k l	θ_h	$\Delta 2\theta_o$	$\Delta 2\theta_c(\Delta\lambda, \delta, t)$	$\Delta 2\theta(\Delta\lambda)$	$\Delta 2\theta(t)$
1 1 1	12.43	0.066	0.066	0.008	0.009
2 0 0	14.39	0.068	0.068	0.009	0.009
2 2 0	20.57	0.064	0.072	0.013	0.009
3 1 1	24.33	0.067	0.075	0.016	0.009
4 0 0	29.80	0.072	0.080	0.020	0.010
3 3 1	32.79	0.074	0.083	0.023	0.010
4 2 2	37.49	0.079	0.087	0.027	0.010
5 1 1	40.21	0.083	0.091	0.030	0.011
5 3 1	47.31	0.096	0.100	0.038	0.012
6 2 0	51.79	0.103	0.108	0.045	0.013
7 1 1	62.53	0.137	0.136	0.067	0.018
7 3 1	72.62	0.199	0.190	0.112	0.028

Table 3. *The average thickness t of the crystallites of* ZnO *in the direction of the diffraction vector* **h**, *calculated using* (7) *for* Cu $K\alpha_1$ *radiation, with* $\Delta\lambda/\lambda = 0.000306$ *and* $\delta = 0.05°$

h k l	θ_h (°)	$\Delta 2\theta$(FWHM) (°)	t_h (Å)
1 0 0	15.88	0.220	539
0 0 2	17.21	0.221	542
1 0 1	18.13	0.242	484
1 0 2	23.77	0.323	352
1 1 0	28.30	0.244	538
1 0 3	31.42	0.299	427
2 0 0	33.19	0.257	539
1 1 2	33.97	0.266	520
2 0 1	34.54	0.275	501
0 0 4	36.28	0.269	533
2 0 2	38.48	0.348	392
1 0 4	40.69	0.427	315
2 0 3	44.80	0.359	427
2 1 0	46.40	0.330	495
2 1 1	47.65	0.342	486
1 1 4	49.30	0.346	499
2 1 2	51.46	0.432	394
1 0 5	52.06	0.429	404
2 0 4	53.71	0.522	330
3 0 0	55.19	0.394	495
2 1 3	58.13	0.476	425
3 0 2	60.78	0.470	476
0 0 6	62.57	0.507	462
2 0 5	66.95	0.680	387
1 0 6	68.25	0.931	282
2 1 4	69.25	0.856	328
2 2 0	71.46	0.706	473

beam is not a constant but varies slightly with the Bragg angle. In Table 2, the experimental widths (third column) are compared with the calculated widths (fourth column). The contributions to the width due to $\Delta\lambda/\lambda$ [first term in (6), fifth column in Table 2] and t [second term in (6), sixth column in Table 2] are also given. It should be noted that the particle-size effect contributes about 10–15% to the total width, even for the standard powder with the coherent domain size $t = 1$ μm.

The middle and upper curves correspond to the widths of the ZnO powder (x in Fig. 4). The middle curve is calculated with $t = 600$ Å and the upper curve with $t = 300$ Å with the two limiting particle sizes obtained from the TEM. In Table 3, the particle

size t_h calculated from (6),

$$t_h = 0.94\lambda/\{\cos\theta_h[\Delta 2\theta(\text{FWHM}) - \delta - 2\Delta\lambda/\lambda \tan\theta_h]\}, \quad (7)$$

is given in the fourth column. Fig. 4, as well as the results given in Table 3, agrees well with the TEM result, confirming the applicability of the approach introduced in this paper.

Discussion

Equation (2) is applicable only to ideal powder samples, *i.e.* for powders consisting of strain-free and preferred-orientation-free crystallites, whose orientations are completely random and the number of which present in the irradiated specimen is very large. Furthermore, it was assumed that extinction and absorption effects can be neglected. Only such an ideal powder is represented in reciprocal space by ideally spherical concentric shells with homogenous thickness and occupation density.

Strain, preferred orientation, large absorption and/or extinction result in deformations of these shells, varying $\mathbf{d}^*$ (strain), ε (absorption, extinction, strain) and the occupation density within the shells (preferred orientation). It will be shown in paper II that all these effects can be represented in reciprocal space and have to be taken properly into account, resulting in general equations analogous to (2).

Concluding remarks

Comparing the width $\Delta\theta_h$ obtained for single-crystal diffractometry, expression (1*b*), with the formula for $\Delta 2\theta$, (6), deduced for powder diffraction, it is obvious that the main difference is introduced by the term corresponding to the size of the coherently scattering particles. The random orientation of the crystallites in the powder results in $\cos\theta_h$ in the denominator of this term, causing appreciable broadening of the Bragg reflections for large Bragg angles only. In single-crystal diffractometry, the crystal is rotated about the θ axis during the scan. This rotation causes $\sin 2\theta_h$ in the denominator of the particle-size term in (1*b*). The rocking curves are therefore broadened appreciably for small as well as for large values of θ_h.

I thank Mrs G. Kumpat and Mr G. Ulrich for preparing the computer graphics of Figs. 1–4.

References

AZAROFF, L. V. (1968). *Elements of X-ray Crystallography*. New York: McGraw-Hill.
BOLIS, V., FUBINI, B., GIAMELLO, E. & RELLER, A. (1989). *J. Chem. Soc. Faraday Trans.* 1, **85**, 855–867.
CAGLIOTI, G., PAOLETTI, A. & RICCI, F. P. (1958). *Nucl. Instrum.* **3**, 223–228.
LADELL, J., ZAGOFSKY, A. & PEARLMAN, S. (1975). *J. Appl. Cryst.* **8**, 499–506.
LANGFORD, J. I., BOULTIF, A., AUFFRÉDIC, J. P. & LOUËR, D. (1993). *J. Appl. Cryst.* **26**, 22–33.
LOUËR, D. & LANGFORD, J. I. (1988). *J. Appl. Cryst.* **21**, 430–437.
RIETVELD, H. M. (1969). *J. Appl. Cryst.* **2**, 65–71.
ROSSMANITH, E. (1992). *Acta Cryst.* **48**, 596–610.
ROSSMANITH, E. (1993*a*). *Acta Cryst.* A**49**, 80–91.
ROSSMANITH, E. (1993*b*). *J. Appl. Cryst.* **26**, 753–755.
ROSSMANITH, E., ADIWIDJAJA, G., ECK, J., KUMPAT, G. & ULRICH, G. (1994). *J. Appl. Cryst.* Submitted.
ROSSMANITH, E., WERNER, M., KUMPAT, G., ULRICH, G. & EICHHORN, K. (1993). *J. Appl. Cryst.* **26**, 756–762.
SABINE, T. M. (1987). *J. Appl. Cryst.* **20**, 23–27, 173–178.
WROBLEWSKI, T. (1991). *Acta Cryst.* A**47**, 571–577.

Acta Cryst. (1994). A**50**, 68–72

A Generalized Patterson-Search Method

BY CHRISTER E. NORDMAN

Department of Chemistry, University of Michigan, Ann Arbor, MI 48109, *USA*

(*Received* 22 *January* 1992; *accepted* 30 *June* 1993)

Abstract

A procedure for Patterson search, or molecular replacement, is described in which the criteria of fit are based on matching the asymmetric unit of the entire Patterson function. In rotation search, the Patterson function is compared with the self-Patterson of the search model; in translation search, the comparison is with the full Patterson function of the search model. Significant features of the method are: (1) all overlaps of vector sets of neighboring molecules are taken into account; (2) all overlaps of the search model with neighboring copies are detected and the evaluation bypassed; and (3) the